BIOCHEMICAL PHARMACOLOGY 74 (2007) 742–751

available at www.sciencedirect.com

ScienceDirect

journal homepage: www.elsevier.com/locate/biochempharm

# Prodelphinidin B-4 3′-O-gallate, a tea polyphenol, is involved in the inhibition of COX-2 and iNOS via the downregulation of TAK1-NF-κB pathway

*De-Xing Hou* [a,*], *Dong Luo* [a], *Shunsuke Tanigawa* [a], *Fumio Hashimoto* [b], *Takuhiro Uto* [a], *Satoko Masuzaki* [a], *Makoto Fujii* [a], *Yusuke Sakata* [b]

[a] *Department of Biochemical Science and Technology, Faculty of Agriculture, Kagoshima University, Korimoto 1-21-24, Kagoshima City 890-0065, Japan*

[b] *Department of Horticultural Science, Faculty of Agriculture, Kagoshima University, Korimoto 1-21-24, Kagoshima City 890-0065, Japan*

ARTICLE INFO

*Article history:*
Received 9 April 2007
Accepted 7 June 2007

*Keywords:*
Proanthocyanidin
COX-2
iNOS
NF-κB
IKKα/β
TAK1

ABSTRACT

Much is known about the bioactive properties of green tea flavan-3-ol. However, very little work has been done to determine the properties of proanthocyanidins, another kind of polyphenols in green tea. In this study, we have investigated the anti-inflammatory effect of tea prodelphinidin B-4 3′-O-gallate (PDG) by demonstrating the inhibitory effects on cyclooxygenase-2 (COX-2) and inducible nitric oxide synthase (iNOS) in lipopolysaccharide (LPS)-activated murine macrophage RAW264 cells. PDG caused a dose-dependent inhibition of COX-2 and iNOS at both mRNA and protein levels with the attendant decrease of prostaglandin $E_2$ ($PGE_2$) and nitric oxide (NO) production. Molecular data revealed that PDG downregulated NF-κB signaling pathway. Electrophoretic mobility shift assay (EMSA) showed that PDG reduced the binding complex of NF-κB–DNA in the promoter of COX-2 and iNOS. Immunochemical analysis revealed that PDG suppressed LPS-induced phosphorylation and degradation of IκBα, and subsequent nuclear translocation of p65. Consequently, PDG suppressed phosphorylation of IκB kinase α/β (IKKα/β) and TGF-β-activated kinase (TAK1). Taken together, our data indicated that PDG is involved in the inhibition of COX-2 and iNOS via the downregulation of TAK1-NF-κB pathway, revealing partial molecular basis for the anti-inflammatory properties of tea PDG.



## 1. Introduction

Prodelphinidin B-4 3′-O-gallate (PDG), one of proanthocyanidins, consists of (+)-gallocatechin and (-)-epigallocatechin 3-O-gallate moieties in a molecule [1] (Fig. 1). Proanthocyanidins are oligomeric and polymeric end products of the flavonoid biosynthetic pathway. They are present in the fruits, bark, leaves and seeds of many plants, especially enriched in tea, grape seed and cranberry [2]. Recently, they are increasingly recognized as having beneficial effects on human health because several lines of evidence showed that they have antioxidant [2,3], antimutagenic [2,4], anticancer [2,5] and

* *Corresponding author*. Tel.: +81 99 285 8649; fax: +81 99 285 8649.
E-mail address: hou@ms.kagoshima-u.ac.jp (D.-X. Hou).

*Abbreviations:* COX-2, cyclooxygenase-2; EMSA, electrophoretic mobility shift assay; IKK, IkappaB kinase; iNOS, inducible nitric oxide synthase; LPS, lipopolysaccharide; NF-κB, nuclear factor kappaB; NO, nitric oxide; PDG, prodelphinidin B-4 3′-O-gallate; $PGE_2$, prostaglandin $E_2$; TAK1, TGF-β-activated kinase; TLR4, toll-like receptor 4

0006-2952/$ – see front matter © 2007 Published by Elsevier Inc.
doi:10.1016/j.bcp.2007.06.006

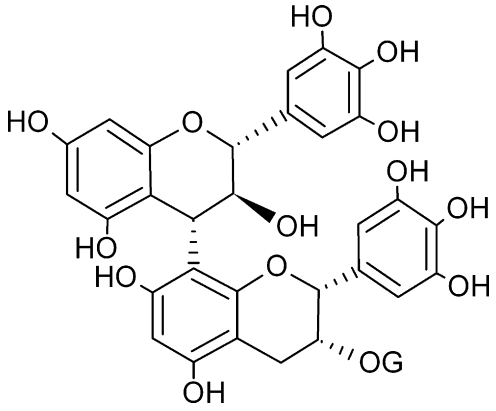


**Fig. 1 – Chemical structures of prodelphinidin B-4 3′-O-gallate (PDG), G; gallate.**

anti-inflammatory activities [2,6]. For example, (+)-catechin, (+)-gallocatechin, and 4′-*O*-methyl-*ent*-gallocatechin isolated from some medicinal plants traditionally used to treat inflammatory conditions, showed inhibitory effects on cyclooxygenase (COX)-2 through measurement of the inhibition of COX-2-catalyzed prostaglandin biosynthesis *in vitro* [6]. However, the underlying mechanisms are not well understood.

COX is a rate-limiting enzyme for synthesis of dienoic eicosanoids such as prostaglandin $E_2$ ($PGE_2$). COX exists in two isoforms [7,8]. COX-1 is expressed constitutively in many types of cells and is responsible for the production of prostaglandins under physiological conditions. COX-2 is induced by pro-inflammatory stimuli, including mitogens, cytokines and bacterial lipopolysaccharide (LPS) in macrophages [8] and epithelial cells [9,10]. Accumulated data indicate that COX-2 is involved in many inflammatory processes and induced in various carcinomas, suggesting that COX-2 plays a key role in inflammation and tumorigenesis [11,12]. Thus, the identification of COX-2 inhibitor is considered to be a promising approach to protect against inflammation and tumorigenesis.

Nitric oxide synthase (NOS) is an enzyme that catalyzes L-arginine to produce nitric oxide (NO). There are three distinct isoforms of NOS. Endothelial nitric oxide synthase (eNOS) and neuronal nitric oxide synthase (nNOS) are constitutively expressed in endothelium and neural tissues, respectively [13]. On the other hand, inducible nitric oxide synthase (iNOS) is only induced by various inflammatory stimuli, such as bacterial endotoxic LPS and inflammatory cytokines in macrophages, hepatocytes and endothelial cells [13–15]. iNOS catalyzes the formation of a large amount of NO, which plays a key role in the various forms of inflammation and carcinogenesis [15–17]. Therefore, NO production by iNOS may reflect the degree of inflammation, and provides a measure to assess the effect of chemopreventive agents on the inflammatory process.

Regarding the regulation of COX-2 and iNOS gene expression, nuclear factor κB (NF-κB), has been identified to bind the *cis*-acting elements in the promoter of COX-2 and iNOS genes, and to regulate their transcription [11,18]. NF-κB is one of the principal inducible transcription factors mediated by many cytokines and inflammatory products such as LPS [19,20]. In most unstimulated conditions, NF-κB is sequestered in the cytosol in an inactive state, NF-κB-IκBs (α or β) complex. When IκBs are phosphorylated and degraded, NF-κB migrates to the nucleus and becomes active form. NF-κB activates a number of rapid response genes involved in the inflammatory response such as COX-2 and iNOS [11,12]. Recent studies indicate that LPS binds toll-like receptor 4 (TLR4) in cellular membrane and mediates a TLR4-mediated NF-κB pathway [21,22]. Although the molecular events are not fully understood in LPS-signaling, TGF-β-activated kinase (TAK1) and IκB kinases (IKK) are suggested to be the two important factors. In unstimulated conditions, TAK1 binds TNF receptor-associated factor 6 (TRAF6) with TAK-binding protein (TAB), and forms a complex of TRAF6/TAK1/TAB1/TAB2 in membrane [21,23]. Phosphorylation of TAK1 initiates the release of the complex from the membrane, and then phosphorylates downstream targets such as the IκB kinases (IKKs). Once activated IKKs subsequently induces phosphorylation and subsequent degradation of IκBs [24,25].

In the present study, we used mouse macrophage cell line RAW264, which can be stimulated with LPS to mimic a state of infection and inflammation, to demonstrate the molecular mechanism of inhibitory action of PDG on COX-2 and iNOS expression. Our data showed that the downregulation of TAK1-NF-κB pathway was involved in the inhibition of COX-2 and iNOS expression by PDG.

## 2. Materials and methods

### 2.1. Materials and cell culture

PDG (Fig. 1) was isolated from tea as described previously [1] with 99% purity, and dissolved in distilled water. Lipopolysaccharide (LPS, *Escherichia coli* Serotype 055:B5) was from Sigma. Antibodies against phospho-TAK1(Thr184/187), phospho-IKKα/β(Ser176/180), phospho-IκB-α(Ser32), and IκB-α were purchased from Cell Signaling Technology, Beverly, MA, USA. Antibodies against COX-2, COX-1, IKKα/β, TAK1, p65 and α-tubulin were from Santa Cruz Biotechnology, CA, USA.

Murine macrophage-like RAW264 cells were obtained from RIKEN BioResource Center Cell Bank (Cell No. RCB0535), Japan, and cultured at 37 °C in a 5% $CO_2$ atmosphere in Dulbecco's modified Eagle's medium (DMEM) containing 10% FBS.

### 2.2. Measurement of $PGE_2$ and nitrite

$PGE_2$ in culture medium was measured with a $PGE_2$ enzyme immunoassay kit (Cayman Co., St. Louis, MO, USA) according to manufacturer's manual [26]. In brief, RAW264 cells ($5 \times 10^5$ cells) were seeded into each well of 6-well plates. After incubation for 24 h, the cells starved by being cultured in serum-free for another 2.5 h to eliminate the influence of FBS. The cells were then treated with or without PDG for 30 min before exposure to 40 ng/ml LPS for 12 h. The amount of $PGE_2$ released into the medium was determined by measuring absorbance at 405 nm with a microplate reader.

Nitrite concentrations were measured by Griess reaction [27]. RAW264 cells ($3 \times 10^5$ cells) were seeded in 48-well plates.

The cells were treated with or without PDG for 30 min before exposure to 40 ng/ml LPS for 12 h. The amount of nitrite in the medium (100 μl) was detected through the reaction with the same volume of Griess reagent (1% sulfanilamide in 5% phosphoric acid and 0.1% *N*-(1-naphthyl) ethylenediamide dihydrocholide in distilled water) for 10 min at room temperature, and the absorbance was measured at 550 nm wavelength.

### 2.3. Protein extraction and Western blotting

RAW264 cells ($6 \times 10^6$) were pre-cultured in 15-cm dish for 24 h, and then starved by being cultured in serum-free for another 2.5 h to eliminate the influence of FBS. The cells were treated with PDG for 30 min before exposure to 40 ng/ml LPS. For whole protein extract, harvested cells were lysed and boiled for 5 min. For nuclear extract, harvested cells were lysed and then centrifuged at 14,000 × *g* for 15 min at 4 °C [26]. After three washes, nuclear pellets were suspended in a buffer containing 20 mM HEPES, 0.5 M KCl, 1 mM EDTA, 1 mM dithiothreitol, 1 mM phenylmethylsulfonyl fluoride, pH 7.9 for 30 min at 4 °C. The nuclear extracts was separated by centrifugation at 14,000 × *g* for 15 min at 4 °C, and then boiled for 5 min.

Western blotting assay was performed as described previously [28]. Protein concentration was determined using dye-binding protein assay kit (Bio-Rad, Hercules, CA, USA) according to the manufacturer's manual. Equal amounts of protein (40 μg) were run on SDS-PAGE and electrophoretically transferred to PVDF membrane (Amersham Pharmacia Biotech). After blotting, the membrane was incubated with specific primary antibody overnight at 4 °C, and further incubated for 1 h with HRP-conjugated secondary antibody. Bound antibodies were detected by ECL system with a Lumi Vision PRO machine (TAITEC, Japan). The relative amount of proteins associated with specific antibody was quantified using the Lumi Vision Imager software.

### 2.4. RNA extraction and RT-PCR

RAW264 ($1 \times 10^6$ cells) was pre-cultured in 6-cm dish for 24 h, and then starved by being cultured in serum-free for another 2.5 h to eliminate the influence of FBS. The cells were treated with or without PDB for 30 min before exposure to 40 ng/ml LPS for 6 h. Total RNA was extracted with an Isogen RNA Kit (Nippon Gene Co., Toyama, Japan) as described in manufacture manual. The PCR primers for mouse *COX-2* [29], *COX-1* [30], *iNOS* [31] and *GAPDH* [32] genes were summarized in Table 1. The RT-PCR was performed with Ready-to-Go RT-PCR beads (Amersham Pharmacia Biotech, Little Chalfont, UK) as described previously [33]. Briefly, RNA (250 ng) was used for reverse-transcription into cDNA at 42 °C for 30 min using oligo (dT) 12–18 primers. Amplifications were done at 95 °C for 30 s, 55 °C for 30 s and 72 °C for 60 s with GenAmp PCR System 2400 machine (Perkin-Elmer). Template- and cycle-dependence of the PCR products were confirmed, and the available cycle numbers of PCR for COX-2, COX-1, iNOS and GAPDH were determined as 30, 30, 33 and 21 cycles, respectively. The PCR products were separated on 2% agarose gel, and digitally imaged after staining ethidium bromide. The bands were quantified with Imager Gauge Software (Fuji Photo Film, Tokyo, Japan). The mRNA level in the control is arbitrarily set to 1.0 as the basal level for subsequent mRNA comparisons.

**Table 1 – Oligonucleiotides used in PCR and EMSA**

| Name | Sequence |
|---|---|
| PCR | |
| COX-2 (490 bp) | 5′-CAG CAA ATC CTT GCT GTT CC-3′<br>5′-TGG GCA AAG AAT GCA AAC ATC-3′ |
| COX-l (450 bp) | 5′-ACT GGC TCT GGG AAT TTG TG-3′<br>5′-AGA GCC GCA GGT GAT ACT GT-3 |
| iNOS (497 bp) | 5′-CCC TTC CGA AGT TTC TGG CAG CAG C-3′<br>5′-GGC TGT CAG AGA GCC TCG TGG CTT TGG-3′ |
| GAPDH (842 bp) | 5′-GAC CCC TTC ATT GAC CTC AAC-3′<br>5′-CAT ACC AGG AAA TGA GCT TG-3′ |
| EMSA | |
| Wild NF-κB | 5′-GAG AGG TGA **GGG GAT TCC** CTT AGT TAG-3′<br>5′-CTA ACT AAG **GGA ATC CCC** TCA CCT CTC-3′ |
| Mutant NF-κB | 5′-GAG AGG TGA **GGG CCT TCC** CTT AGT TAG-3′<br>5′-CTA ACT AAG **GGA AGG CCC** TCA CCT CTC-3′ |

### 2.5. Electrophoretic mobility shift assay (EMSA)

EMSA was performed as described previously [34]. In brief, oligonucleotide probes (Table 1) were synthesized by Genenet Co. (Fukuoka, Japan), and then annealed in TE buffer. Ten pmol probes were labeled with T4 polynucleotide kinase (Takara Bio, Siga, Japan) and [$\gamma$-$^{32}$P] ATP (5000 Ci/mmol; Amersham Biosciences). The labeled oligonucleotides were purified using a SephadexG-25 spin column (Amersham Biosciences). Five μg of nuclear extract was incubated at 25 °C for 30 min with labeled or unlabeled competitor oligonucleotides in binding buffer (25 mM Tris–HCl, pH 7.5, 75 mM KCl, 0.3% Nonidet-40, 7.5% glycerol, 2.5 mM dithiothreitol, 1 mg/ml bovine serum albumin and 1 μg of poly(dI)·poly(dC)). The products were electrophoresed at 4 °C on a 5% nondenaturing polyacrylamide gel in 0.5 × Tris borate/EDTA buffer, and the gel was then dried on chromatography paper. The radioactivity on paper was detected with FLA-2000 machine (Fuji Photo Film, Tokyo, Japan).

### 2.6. Statistical analyses

Difference between the treated and the control was analyzed by Student's *t*-test. A probability of $P < 0.05$ was considered significant.

## 3. Results

### 3.1. PDG suppresses COX-2 expression and $PGE_2$ release

To examine the inhibitory effect of PDG on COX-2 expression, RAW264 cells were treated with the indicated concentrations of PDG for 30 min before exposure to 40 ng/ml LPS for 12 h. As shown in Fig. 2A, PDG suppressed LPS-induced expression of COX-2, but not COX-1, in a dose-dependent manner at the concentration range of 25–75 μM. Furthermore, PDG also

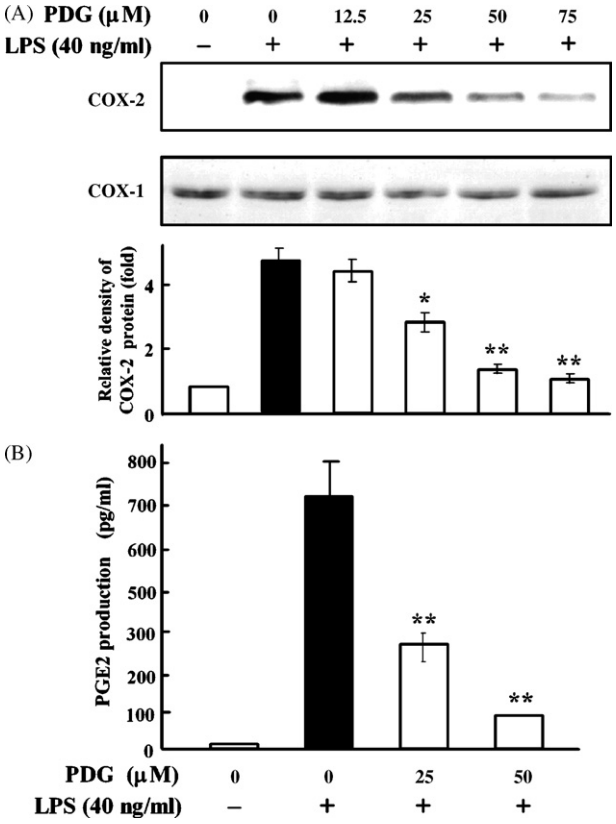


**Fig. 2 – PDG inhibits LPS-induced COX-2 protein and $PGE_2$ release in RAW264 cells. (A) COX-2 detection. After RAW264 cells ($1 \times 10^6$ cells) were starved in serum-free medium for 2.5 h, the cells were treated with the indicated concentrations of PDG for 30 min, and then exposed to 40 ng/ml LPS for 12 h. COX-2 and COX-1 were detected by Western blotting with their antibodies, respectively. Histograms show the densitometric analysis of COX-2 protein normalized to COX-1. The data represent the mean ± S.D. of three to four separate experiments. (B) $PGE_2$ measurement. After RAW264 cells ($5 \times 10^5$ cells) were starved in serum-free medium for 2.5 h, the cells were treated with the indicated concentrations of PDG for 30 min, and then exposed to 40 ng/ml LPS for 12 h. The amount of $PGE_2$ in medium was measured as described in Section 2. Each value represents the mean ± S.D. of triplicate tests. $^{*}P < 0.05$; $^{**}P < 0.01$ vs. LPS alone.**

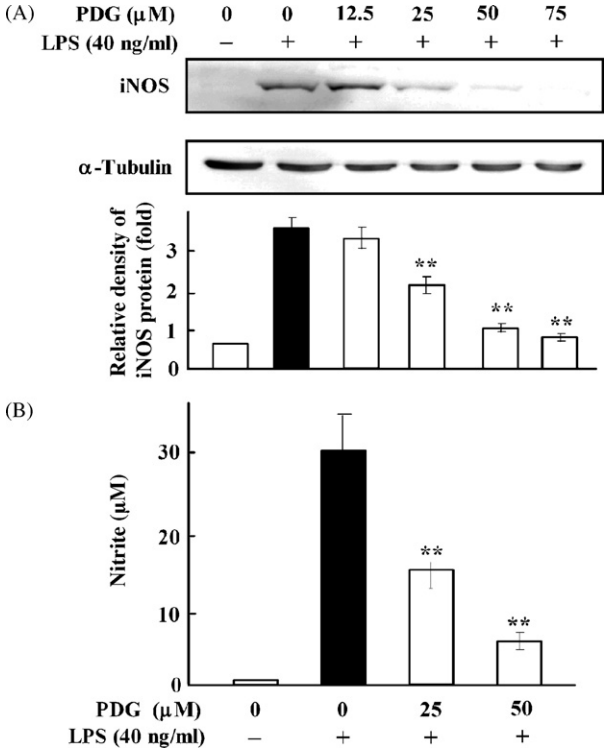


**Fig. 3 – PDG inhibits LPS-induced iNOS protein and NO production. (A) iNOS detection. Cell culture and PDG treatment were done as described in Fig. 2A. iNOS and α-tubulin were detected with their antibodies, respectively. Histograms show the densitometric fold of iNOS protein normalized to α-tubulin. (B) Nitrite concentration measurement. RAW264 cells ($3 \times 10^5$ cells) were pretreated with 25–50 μM of PDG for 30 min, and then exposed to 40 ng/ml LPS for 12 h. The culture medium was subsequently isolated and nitrite concentration was determined by Griess reaction. Each value represents the mean ± S.D. of triplicate tests. $^{**}P < 0.01$ vs. LPS alone.**

suppressed LPS-induced $PGE_2$ release with the same fashion of COX-2 protein (Fig. 2B). The inhibitory action by PDG was not caused by their cytotoxicity because the concentration that suppressed COX-2 protein did not affect cell viability as measured by Trypan blue assay (data not shown). These results indicate that PDG may be a potential inhibitor for COX-2.

### 3.2. *PDG suppresses iNOS expression and NO production*

It has been reported that LPS also can induce iNOS expression and NO release [13–15]. Thus, we next examined the effect of PDG on LPS-induced iNOS protein and nitrite production in such treatment. As shown in Fig. 3A, PDG suppressed LPS-induced iNOS protein in a dose-dependent manner at the concentration range of 25–75 μM. As a control, α-tubulin showed no change in such treatment. Furthermore, PDG also suppressed LPS-induced nitrite production with the same fashion of iNOS protein (Fig. 3B).

### 3.3. *PDG downregulates mRNA levels of COX-2 and iNOS*

It has been reported that LPS maximally increased the COX-2 and iNOS mRNA at 6–12 h [35,36]. To determine whether PDG suppresses LPS-induced COX-2 and iNOS mRNA, we examined their mRNA levels at 6 h by RT-PCR. The results showed that PDG inhibited LPS-induced increase in both COX-2 (Fig. 4A) and iNOS mRNA (Fig. 4B) at the concentration range of 25–75 μM while PDG had no effect on COX-1 mRNA level in such treatment. GAPDH mRNA as control showed no change (Fig. 4B). These data revealed that PDG also suppressed LPS-induced increase in COX-2 and iNOS mRNA, although we could not rule out whether the increases in mRNA levels was partially due to increases in mRNA stability.

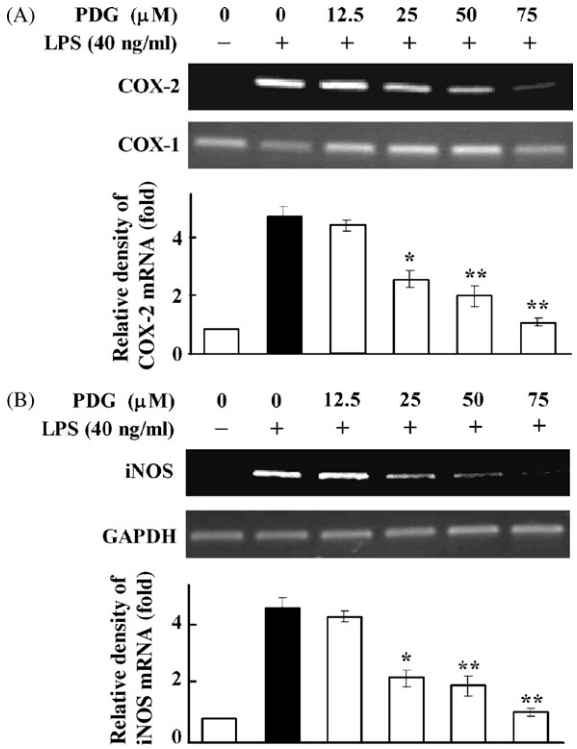


**Fig. 4 – PDG downregulates mRNA levels of COX-2 (A) and iNOS (B). RAW264 cells ($1 \times 10^6$ cells) were starved in serum-free medium for 2.5 h, the cells were then treated with the indicated concentration of PDG for 30 min before exposure to 40 ng/ml LPS for 6 h. RNA was extracted with Isogen RNA isolation kit and COX-2 and COX-1 mRNA were detected by RT-PCR. The RT-PCR products were separated on 2% agarose gel, and digitally imaged after staining with ethidium bromide. Quantification of the bands was performed using Imager Gauge Software. Histograms show the densitometric fold of COX-2 mRNA normalized to COX-1 mRNA, and of iNOS mRNA normalized to GAPDH. Each value represents the mean ± S.D. of three to four separate experiments. $^{*}P < 0.05$; $^{**}P < 0.01$ vs. LPS alone.**

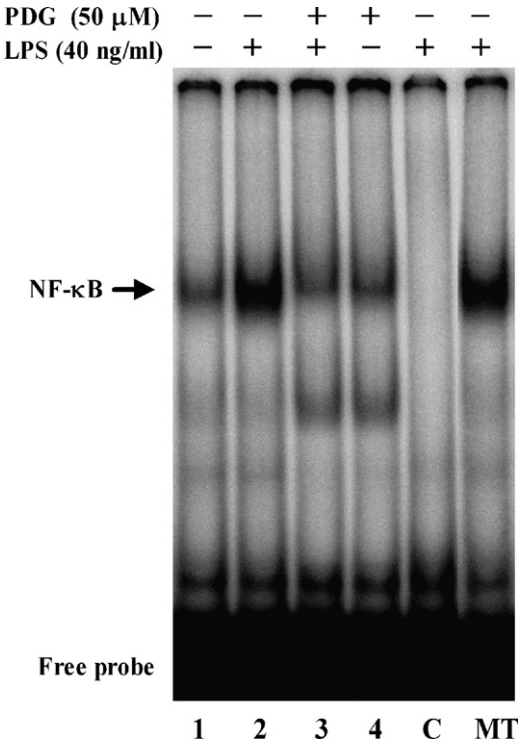


**Fig. 5 – PDG reduces the binding complex of NF-κB–DNA. RAW264 cells was pretreated with vehicle or 50 μM PDG for 30 min, and then exposed to 40 ng/ml LPS for another 30 min. Nuclear protein was extracted and then incubated with labeled wild NF-κB probe (lane 1–4), 10-fold excess molar of cold NF-κB oligonucleotides (lane C) or labeled mutant NF-κB probe (lane MT). After separated by 5% nondenaturing polyacrylamide gel, the gel was dried on 3 MM chromatography paper and exposed to a radioactive imaging plate. The signal was detected with FLA-2000 machine.**

### 3.4. *PDG reduces the binding complex of NF-κB–DNA*

Accumulated data indicate that NF-κB is one of the principal factors for COX-2 and iNOS expression mediated by LPS or proinflammatory cytokines [19,20]. Thus, we hypothesize that NF-κB signaling pathway may be involved in PDG-mediated inhibition of COX-2 and iNOS. To demonstrate this, we used 50 μM PDG, which is proven to be efficient concentration without cytotoxicity in our experiments, to examine NF-κB signaling pathway at different times dependent on signaling factors.

First, we examined the binding complex of NF-κB to the promoter of COX-2 and iNOS by EMSA with NF-κB specific $^{32}$P-labeled oligonucleotides, which are derived from original NF-κB binding sequences in the promoter of mouse COX-2 [11], and the NF-κB core sequences are also found in the promoter of mouse iNOS [37]. As indicated in Fig. 5, LPS caused a marked increase in binding complex of NF-κB–DNA (lane 2). Pretreatment with 50 μM PDG reduced the binding complex of NF-κB–DNA induced by LPS (lane 3). PDG alone showed no change (lane 4). The specific interaction between DNA and NF-κB was demonstrated by competitive inhibition with excess unlabelled and mutant NF-κB oligonucleotides. Treatment with 10-fold excess unlabled NF-κB oligonucleotides completely blocked the binding complex (lane C) while treatment with excess mutant NF-κB oligonucleotides did not block the binding complex (lane MT). These results indicated that PDG might suppress expression of *COX-2* and *iNOS* genes by blocking the binding complex of NF-κB–DNA in their promoter.

### 3.5. *PDG suppresses IκB degradation and p65 translocation*

NF-κB is inactive in the cytosol via binding to IκB and become active through phosphorylation and degradation of IκB and subsequent nuclear translocation of NF-κB preceded by LPS [38,39]. Thus, we next examined whether PDG inhibits phosphorylation and degradation of IκB. RAW 264 cells were pretreated with 50 μM PDG for 30 min and then treated with

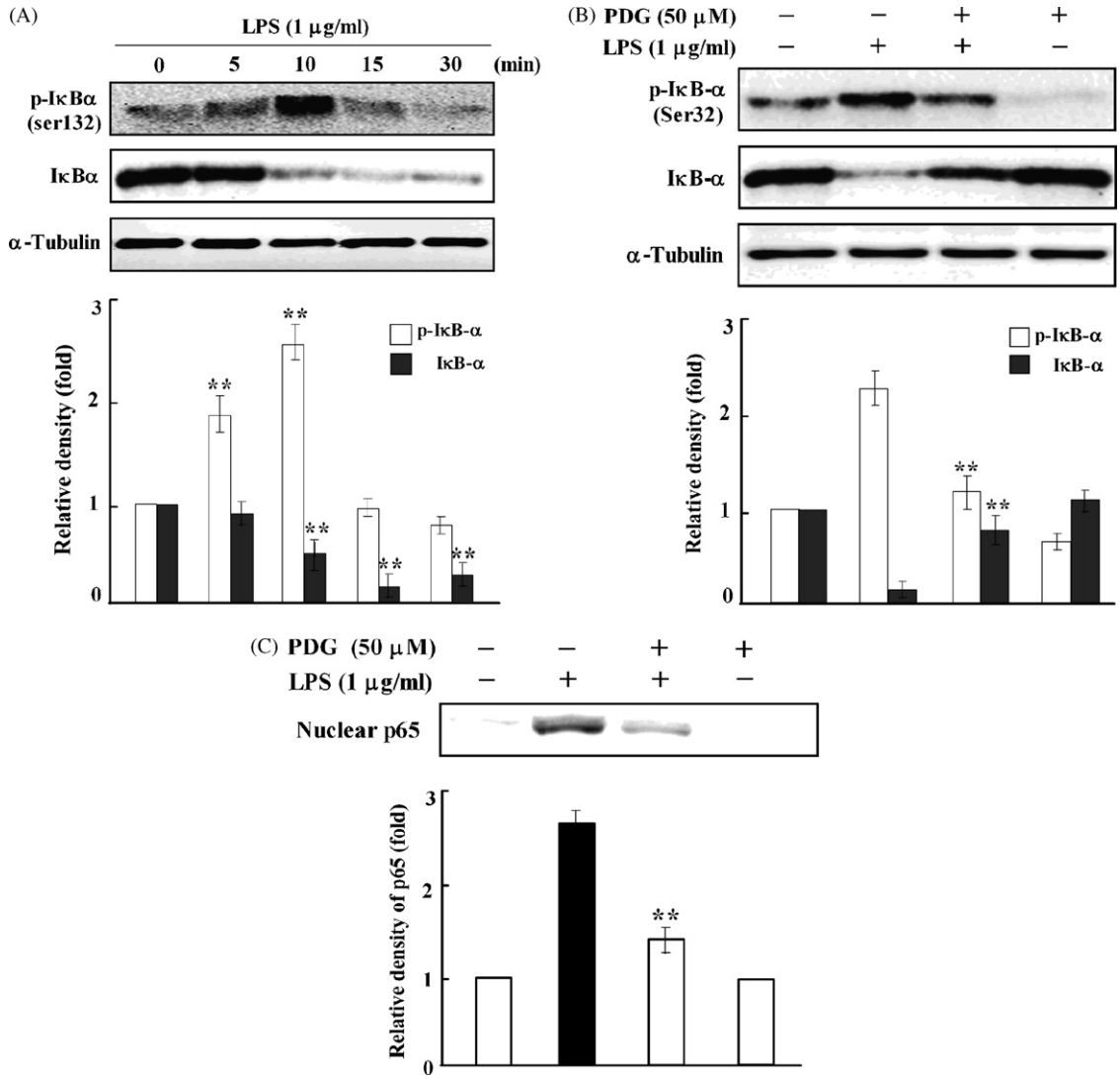


**Fig. 6 – PDG suppresses phosphorylation and degradation of IκB-α and nuclear translocation p65. (A) To identify the time of phosphorylation and degradation of IκB-α induced by LPS, RAW264 cells were treated with 1 μg/ml LPS for 5–30 min. $^{**}P < 0.01$ vs. 0 min. (B) To determine the effect of PDG on phosphorylation and degradation of IκB-α, RAW264 cells were pretreated with 50 μM PDG for 30 min, and then exposed to 1 μg/ml LPS for 10 min. p-IκB-α, IκB-α and α-tubulin were detected with their antibodies, respectively. Histograms show the densitometric fold of p-IκB-α and IκB-α to control normalized to α-tubulin. $^{**}P < 0.01$ vs. LPS alone. (C) For nuclear translocation of p65. Cell culture was performed as Fig. 6B and nuclear protein was extracted. Nuclear p65 were detected with p65 antibody. Histograms show the densitometric fold of p65 in nuclear lysates. The data represent the mean ± S.D. of three separate experiments. $^{**}P < 0.01$ vs. LPS alone.**

40 ng/ml or 1 μg/ml LPS for different times. We found that treatment with 40 ng/ml LPS induced a low expression of proteins in NF-IκB pathway [40]. To clarify the induction of proteins by LPS, we treated the cells with 1 μg/ml LPS as recommended by another group [41]. The results in a time-course experiment revealed that LPS caused phosphorylation and degradation of IκB-α protein at 5–10 min (Fig. 6A, lane 2–3). Thus, we next pretreated the cells with 50 μM PDG for 30 min and then detected IκB-α protein after 10 min exposure to 1 μg/ml LPS. PDG significantly suppressed LPS-induced phosphorylation and degradation of IκB-α (Fig. 6B, lane 3). These results suggest that PDG might inhibit NF-κB activation by blocking LPS-induced IκB-α phosphorylation and degradation. To confirm this, we further examined the nuclear translocation of p65, a part of p65/p50 heterodimer at the same time. In parallel with the result of IκB-α degradation, LPS markedly resulted in p65 translocation from the cytosol to the nucleus after 10 min treatment (Fig. 6C, lane 2), and PDG (50 μM) significantly suppressed the nuclear translocation of p65 (Fig. 6C, lane 3).

### 3.6. *PDG suppresses IKK and TAK1 phosphorylation*

Recent studies have showed that phosphorylation of IκBs is regulated by IκB kinases, IKKα and IKKβ[24,25]. Phosphorylation of IKKα/β is further regulated by upstream factors such as

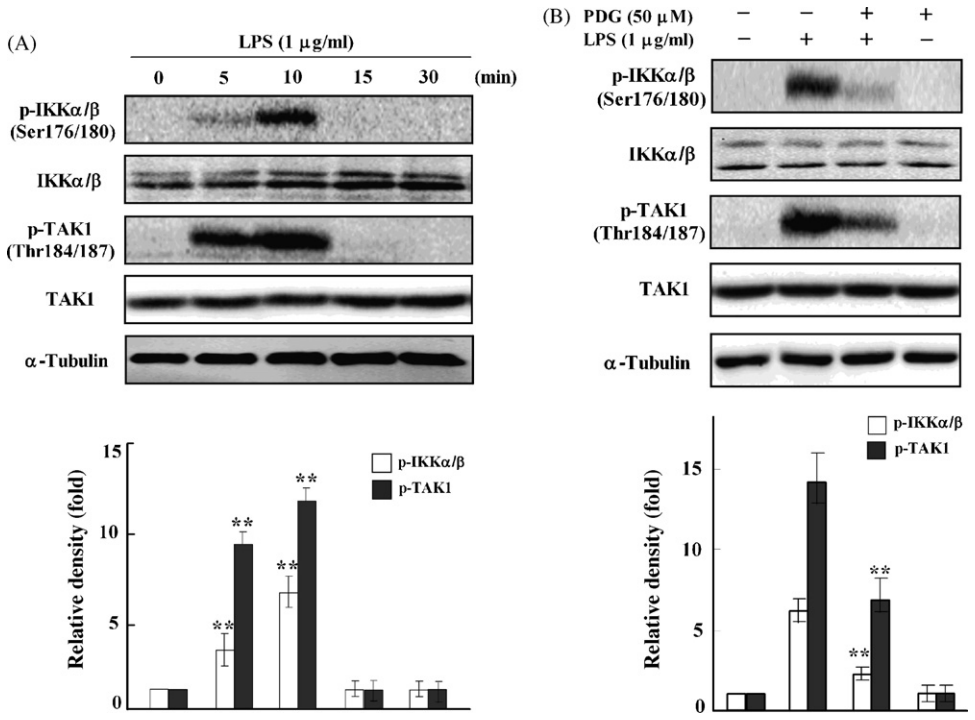


**Fig. 7 – PDG suppresses phosphorylation of IKKα/β and TAK1. (A) To identify the time of phosphorylation of IKKα/β and TAK1 induced by LPS, RAW264 cells were treated with 1 μg/ml LPS for 5–30 min. $^{**}P < 0.01$ vs. 0 min. (B) To determine the effect of PDG on phosphorylation of IKKα/β and TAK1, RAW264 cells were pretreated with 50 μM PDG for 30 min, and then exposed to 1 μg/ml LPS for 10 min. p-IKKα/β, IKKα/β, p-TAK1, TAK1 and α-tubulin were detected with their antibodies, respectively. Histograms show the densitometric fold of phosphorylated IKKα/β and TAK1 to total IKKα/β and TAK1 normalized to α-tubulin, respectively. The data represent the mean ± S.D. of three separate experiments. $^{**}P < 0.01$ vs. LPS alone.**

TAK1 [21–23]. Phosphorylated TAK1 can phosphorylate the IKK complex, which in turn phosphorylates IκB for degradation. Thus, we investigated the effect of PDG on phosphorylation of IKKα/β and TAK1. First, we performed a time-course experiment to determine the time of phosphorylation of IKKα/β and TAK1 induced by LPS. In parallel with the results of phosphorylation and degradation of IκB-α, LPS caused phosphorylation of IKKα/β and TAK1 at 5–10 min (Fig. 7A, lanes 2 and 3), but did not affect total IKKα/β and TAK1 protein. Next, we pretreated the cells with 50 μM PDG for 30 min and then exposed to 1 μg/ml LPS for 10 min. As shown in Fig. 7B, treatment with PDG significantly inhibited phosphorylation of IKKα/β and TAK1 induced by LPS (Fig. 7B, lane 3), but did not affect total IKKα/β and TAK1 protein. The data showed that PDG suppressed TAK1-mediated phosphorylation of IKKα/β and IκB-α.

## 4. Discussion

Proanthocyanidins enriched in tea, grape seed and cranberry have been discussed in relation to anti-inflammation activity [2,6]. However, the molecular targets and the mechanisms underlying their biological activity are poorly defined. In this study, we investigated the effect of PDG on expression of COX-2 and iNOS, which are two molecular targets proven for inflammation responses. Our data showed that PDG caused a dose-dependent inhibition of COX-2 and iNOS at both mRNA and protein, with the attendant reduction of $PGE_2$ and NO.

Multiple lines of evidence have demonstrated that NF-κB plays a critical role in COX-2 and iNOS expression induced by many cytokines and inflammatory products such as LPS [19,20]. NF-κB is composed mainly of two proteins: p65 and p50. In unstimulated cells, NF-κB exists in the cytosol in a quiescent form bound to its inhibitory protein, IκB protein [21,22]. Upon stimulation with LPS, IκB protein become phosphorylated and goes under proteolytic degradation, following this NF-κB translocates to the nucleus where it can activate certain genes including COX-2 and iNOS through binding to transcription-regulatory elements in a nucleotide sequence-specific manner [11,12]. To identify the mechanisms involved in the inhibition of PDG on COX-2 and iNOS expression, we investigated the transcriptional regulation of NF-κB. EMSA data revealed that PDG inhibited the binding complex of NF-κB–DNA present in the *COX-2* and *iNOS* promoter (Fig. 5). Western blotting results revealed that PDG inhibited LPS-induced phosphorylation and degradation of IκBα (Fig. 6A), and the subsequent reduction of p65, a subunit of NF-κB, in nuclear (Fig. 6B). These data suggest that the inhibition of NF-κB activation by PDG might be the results of the inhibition of IκBα phosphorylation and degradation, and then reduction of p65 nuclear translocation. Recent studies

have shown that phosphorylation of IκB is regulated by both $\alpha$ and $\beta$ isoforms of IKK [24,25], which is further regulated by upstream factor such TAK1 [23]. These kinases may represent novel sites for pharmacological intervention in a number of inflammatory conditions. Therefore, we examined the inhibitory effects of PDG on phosphorylation of IKK $\alpha/\beta$ and TAK1. In parallel with the result of IκB-α degradation, PDG also inhibited phosphorylation of IKK $\alpha/\beta$ and TAK1 (Fig. 7). These data indicated that PDG might suppress NF-κB activation through downregulation of TAK1-mediated NF-κB pathway in LPS-activated RAW 264.7 cells.

Accumulated data showed that LPS is recognized by toll-like receptor (TLR4), a member of the TLR family that is involved in innate immunity and inflammation response. Upon binding of TLR4 to LPS, the cytoplasmic region of TLR4 recruits MyD88, which links TLR4 to IRAK1 [21,22]. IRAK1 binds TRAF6, which in turn binds a pre-formed membrane bound complex of TAB1/TAK1/TAB2. Phosphorylation of TAK1 initiates the release of the complex from the membrane, and active TAK1 phosphorylates the IKK complex, which in turn phosphorylates IκB for degradation [21–23]. Our data showed that PDG suppressed TAK1 phosphorylation and subsequent downstream events, such as phosphorylation of IKKα/β and IκB-α. On the other hand, TAK1 is also upstream of LPS-induced MAP kinase activation. MAP kinases including ERK, JNK and p38 can phosphorylate several transcription factors such as c-Jun and c-Fos, and then stimulate AP-1 activation. AP-1 activation has been demonstrated to stimulate COX-2 and iNOS expression [42]. Thus, it is possible that PDG inhibit COX-2 and iNOS expression also through the suppression of TAK1-mediated MAPK activation, although it needs to be confirmed in further study.

The question is what is the upstream molecule targeted by PDG. For this, we investigated whether PDG competitively binds the TLR4 with FITC-conjugated LPS by flow cytometric assay. The results revealed that PDG did not affect LPS-TLR4 binding (Hou et al., unpublished data). Interestingly, ROS has also been reported to be involved in LPS-induced NF-κB activation [43,44]. Pretreatment of neutophils with *N*-acetyl cysteine or α-tocophenol prevented LPS-induced NF-κB activation [44]. Sanlioglu et al. have reported that the activation of Rac1 and subsequent production of ROS are key steps involved in NF-κB activation in macrophage challenged with LPS [45]. Additionally, PDG have shown antioxidant activity in cell-free assay [46]. Based on our data and information of NF-κB signaling, we considered that PDG may target the molecules between TLR4 and TAK1, and ROS and Rac1 may be candidate targets, which are worthy of further investigation.

In this study, we found that PDG might have anti-inflammatory effect by inhibiting COX-2 and iNOS expression. PDG is one of proanthocyanidins in tea. We have isolated six kinds of proanthocyanidins from tea including procyanidin B-2 3, 3′-G, EGCG (4β-8) ECG, prodelphinidin B-2 3, 3′-G, procyanidin B-3, prodelphinidin B-4, prodelphinidin B-4 3′-G, and procyanidin C-1 [1]. The total amounts of proanthocyanidins in tea have been also determined from 2.5 to 9.0 mg/g tea, depending on tea breed [1]. Our data make proanthocyanidins useful tea compounds for further evaluation as a potential anti-inflammatory reagent, although it appears hard to get the concentration shown in this study from daily consumed tea. Work still needs to be done to assess whether there are synergic effects on the inhibition of COX-2 and iNOS between proanthocyanidins and other tea polyphenols.

In summary, we showed that PDG inhibited LPS-induced expression of COX-2 and iNOS with the attendant reduction of $PGE_2$ and NO production. Molecular data revealed that PDG is involved in the inhibition of COX-2 and iNOS via the down-regulation of TAK1-NF-κB pathway. These findings provide partial molecular basis for the anti-inflammatory properties of tea PDG.

## Acknowledgements

This work was supported partly by grant-in-aid for scientific research (C) of the Ministry of Education, Culture, Sports, Science and Technology (MEXT) of Japan (18580125), and partly by the fund of Frontier Science Research Center of Kagoshima University to D.-X., Hou.

## REFERENCES

[1] Hashimoto F, Nonaka G, Nishioka I. Tannins and related compounds. XC. 8-C-ascorbyl (-)-epigallocatechin 3-O-gallate and novel dimeric flavan-3-ols, oolonghomobisflavans A and B, from oolong tea (3). Chem Pharm Bull 1989;37:3255–63.
[2] Dixon RA, Xie DY, Sharma SB. Proanthocyanidins-a final frontier in flavonoid research? New Phytologist 2005; 165:9–28.
[3] Bagchi D, Bagchi M, Stohs SJ, Das DK, Ray SD, Kuszynski CA, et al. Free radicals and grape seed proanthocyanidn extract: importance in human health and disease prevention. Toxicol 2000;148:187–97.
[4] Dauer A, Hensel A, Lhoste E, Knasmueller S, Mersch SV. Genotoxic and antigenotoxic effects of catechin and tannins from the bark of *Hamamelis virginiana* L. in metabolically competent, human hepatoma cells (Hep G2) using single cell gel electrophoresis. Phytochem 2003;63:199–207.
[5] Kandil FE, Smith MAL, Rogers RB, Pepin MF, Song LL, Pezzuto JM, et al. Composition of a chemopreventive proanthocyanidinrich fraction from cranberry fruits responsible for the inhibition of 12-Otetradecanoyl phorbol-13-acetate (TPA)-induced ornithine decarboxylase (ODC) activity. J Agric Food Chem 2002;50:1063–9.
[6] Noreen Y, Serrano G, Perera P, Bohlin L. Flavan-3-ols isolated from some medicinal plants inhibiting COX-1 and COX-2 catalyzed prostaglandin biosynthesis. Planta Med 1998;64:520–4.
[7] Funk CD, Funk LB, Kennedy ME, Pong AS, Fitzgerald GA. Human platelet/erythroleukemia cell prostaglandin G/H synthase: cDNA cloning, expression, and gene chromosomal assignment. FASEB J 1991;5:2304–12.
[8] Hempel SL, Monick MM, Hunninghake GW. Lipopolysaccharide induces prostaglandin H synthase-2 protein and mRNA in human alveolar macrophages and blood monocytes. J Clin Invest 1994;93:391–6.
[9] Kelley DJ, Mestre JR, Subbaramaiah K, Sacks PG, Schantz SP, Tanabe T, et al. Benzo[a]pyrene up-regulates

cyclooxygenase-2 gene expression in oral epithelial cells. Carcinogenesis 1997;18:795–9.
[10] Mitchell JA, Belvisi MG, Akarasereenont P, Robbins RA, Kwon OJ, Croxtall J, et al. Induction of cyclooxygenase-2 by cytokines in human pulmonary epithelial cells: regulation by dexamethasone. Br J Pharmacol 1994;113:1008–14.
[11] Hla T, Ristimaki A, Appleby S, Barriocanal JG. Cyclooxygenase gene expression in inflammation and angiogenesis. Ann NY Acad Sci 1993;696:197–204.
[12] Mestre JR, Chan G, Zhang F, Yang EK, Sacks PG, Boyle JO, et al. Inhibition of cyclooxygenase-2 expression. An approach to preventing head and neck cancer. Ann NY Acad Sci 1999;889:62–71.
[13] Nathan C, Xie QW. Nitric oxide synthases: roles, tolls, and controls. Cell 1994;78:915–8.
[14] Alderton WK, Cooper CE, Knowles RG. Nitric oxide synthases: structure, function and inhibition. Biochem J 2001;357:593–615.
[15] MacMicking J, Xie QW, Nathan C. Nitric oxide and macrophage function. Annu Rev Immunol 1997;15:323–50.
[16] Maeda H, Akaike T. Nitric oxide and oxygen radicals in infection, inflammation, and cancer. Biochemistry 1998;63:854–65.
[17] Lala PK, Chakraborty C. Role of nitric oxide in carcinogenesis and tumour progression. Lancet Oncol 2001;2:149–56.
[18] Xie QW, Kashiwabara Y, Nathan C. Role of transcription factor NFkappa B/Rel in induction of nitric oxide synthase. J Biol Chem 1994;269:4705–8.
[19] D'Acquisto F, Iuvone T, Rombola L, Sautebin LD, Rosa M, Carnuccio R. Involvement of NF-kappaB in the regulation of cyclooxygenase-2 protein expression in LPS-stimulated J774 macrophages. FEBS Lett 1997;418:175–8.
[20] Inoue H, Tanabe T. Transcriptional role of the nuclear factor kappa B site in the induction by lipopolysaccharide and suppression by dexamethasone of cyclooxygenase-2 in U937 cells. Biochem Biophys Res Commun 1998;244: 143–8.
[21] Doyle SL, O'Neill LAJ. Toll-like receptors: from the discovery of NF-κB to new insights into transcriptional regulations in innate immunity. Biochem Pharmacol 2006;72:1102–13.
[22] Gloire G, Legrand-Poels S, Piette J. NF-kB activation by reactive oxygen species: fifteen years later. Biochem Pharmacol 2006;72:1493–505.
[23] Wang C, Deng L, Hong M, Akkaraju GR, Inoue J, Chen ZJ. TAK1 is a ubiquitin-dependent kinase of MKK and IKK. Nature 2001;412:346–51.
[24] Mercurio F, Zhu H, Murray BW, Shevchenko A, Bennett BL, Li J, et al. IKK-2: cytokine-activated IkappaB kinases essential for NF-kappaB activation. Science 1997;278: 860–6.
[25] Regnier CH, Song HY, Gao X, Goeddel DV, Cao Z, Rothe M. Identification and characterization of an IkappaB kinase. Cell 1997;90:373–83.
[26] Uto T, Hou DX, Fujii M. Inhibition of lipopolysaccharide-induced cyclooxygenase-2 transcription by 6-(methylsulfinyl) hexyl isothiocyanate, a chemopreventive compound from *Wasabia japonica (Miq.)* Matsumura, in mouse macrophages. Biochem Pharmacol 2005;70: 1772–84.
[27] Uto T, Hou DX, Fujii M. 6-(Methylsulfinyl)hexyl isothiocyanate suppresses inducible nitric oxide synthase expression through the inhibition of Janus kinase 2-mediated JNK pathway in lipopolysaccharide-activated murine macrophages. Biochem Pharmacol 2005;70: 1211–21.
[28] Hou DX, Kai K, Li JJ, Lin S, Terahara N, Wakamatsu M, et al. Anthocyanidins inhibit activator protein 1 activity and cell transformation: structure-activity relationship and molecular mechanisms. Carcinogenesis 2004;25:29–36.
[29] Sun LK, Beck-Schimmer B, Oertli B, Wuthrich RP. Hyaluronaninduce cyclooxygenase-2 expression promotes thromboxane A2 production by renal cells. Kidney Int 2001;59:190–6.
[30] Chen JC, Huang KC, Wingerd B, Wu WT, Lin WW. HMG-CoA reductase inhibitors induce COX-2 gene expression in murine macrophages: role of MAPK cascades and promoter elements for CREB and C/EBPbeta. Exp Cell Res 2004;301:305–19.
[31] Lo AH, Liang YC, Lin-Shiau SY, Ho CT, Lin JK. Carnosol, an antioxidant in rosemary, suppresses inducible nitric oxide synthase through down-regulating nuclear factor-κB in mouse macrophages. Carcinogenesis 2002;23:983–91.
[32] Sabath DE, Broome HE, Prystowsky MB. Glyceraldehyde-3-phosphate dehydrogenase mRNA is a major interleukin 2-induced transcript in a cloned T-helper lymphocyte. Gene 1990;91:185–91.
[33] Hou DX, Fukuda M, Fujii M, Fuke Y. Transcriptional regulation of nicotinamide adenine dinucleotide phosphate: quinone oxidoreductase in murine hepatoma cells by 6-(methylsufinyl) hexyl isothiocyanate, an active principle of wasabi (*Eutrema Wasabi Maxim.*). Cancer Lett 2000;161:195–200.
[34] Akimaru H, Hou DX, Ishii S. *Drosophila* CBP is required for dorsal-dependent *twist* gene expression. Nat Genet 1997;17:211–4.
[35] Lee AK, Sung SH, Kim YC, Kim SG. Inhibition of lipopolysaccharide-inducible nitric oxide synthase, TNF-α and COX-2 expression by sauchinone effects on I-κBα phosphorylation, C/EBP and AP-1 activation. Br J Pharmacol 2003;139:11–20.
[36] Takahashi F, Takahashi K, Maeda K, Tominaga S, Fukuchi Y. Osteopontin is induced by nitric oxide in Raw264.7 cells. IUBMB Life 2000;49:217–21.
[37] Xie QW, Whisnant R, Nathan C. Promoter of the mouse gene encoding calcium-independent nitric oxide synthase confers inducibility by interferon 3/and bacterial lipopolysaccharide. J Exp Med 1993;177:1779–84.
[38] Baeuerle PA, Baltimore D. I kappa B: a specific inhibitor of the NF-kappa B transcription factor. Science 1988;242:540–6.
[39] Zandi E, Rothwarf DM, Delhase M, Hayakawa M, Karin M. The IkappaB kinase complex (IKK) contains two kinase subunits, IKKalpha and IKKbeta, necessary for IkappaB phosphorylation and NF-kappaB activation. Cell 1997;91:243–52.
[40] Hou DX, Yanagita T, Uto T, Masuzaki S, Fujii M. Anthocyanidins inhibit cyclooxygenase-2 expression in LPS-evoked macrophages: structure-activity relationship and molecular mechanisms involved. Biochem Pharmacol 2005;70:417–25.
[41] Kim Y, Moon JS, Lee KS, Park SY, Cheong J, Kang HS, et al. Ca2+/calmodulin-dependent protein phosphatase calcineurin mediates the expression of iNOS through IKK and NF-kappaB activity in LPS-stimulated mouse peritoneal macrophages and RAW 264.7 cells. Biochem Biophys Res Commun 2004;314:695–703.
[42] Janssens S, Beyaert R. Functional diversity and regulation of different interleukin-1 receptor-associated kinase (IRAK) family members. Mol Cell 2003;11:293–302.
[43] Asehnoune K, Strassheim D, Mitra S, Kim JY, Abraham E. Involvement of reactive oxygen species in Toll-like receptor 4-dependent activation of NF-kappa B. J Immunol 2004;172:2522–9.
[44] Ryan KA, Smith Jr MF, Sanders MK, Ernst PB. Reactive oxygen and nitrogen species differentially regulate Toll-like receptor 4-mediated activation of NF-kappa B and

interleukin-8 expression. Infect Immun 2004;72:2123–30.
[45] Sanlioglu S, Williams CM, Samavati L, Butler NS, Wang G, McCray Jr PB, et al. Lipopolysaccharide induces Rac1-dependent reactive oxygen species formation and coordinates tumor necrosis factor-alpha secretion through IKK regulation of NF-kappa B. J Biol Chem 2001;276:30188–9.
[46] Hashimoto F, Ono M, Masuoka C, Ito Y, Sakata Y, Shimizu K, et al. Evaluation of the anti-oxidative effect (*in vitro*) of tea polyphenols. Biosci Biotechnol Biochem 2003;67:396–401.